Asian Journal of Chemistry; Vol. 27, No. 2 (2015), 690-696

ASIAN JOURNAL OF CHEMISTRY

http://dx.doi.org/10.14233/ajchem.2015.17772

Comparative Study of Coconut Shell and Palm Kernel Shell Biomass as Adsorbents for Sorption of Pb^{2+} from Aqueous Solution

DONBEBE WANKASI and EZEKIEL DIXON DIKIO*

Applied Chemistry and Nano-Science Laboratory, Department of Chemistry, Vaal University of Technology, P.O. Box X021, Vanderbijlpark 1900, South Africa

*Corresponding author: E-mail: ezekield@vut.ac.za

Received: 7 April 2014; *Accepted*: 24 June 2014; *Published online*: 10 January 2015; AJC-16647

A comparative study of the sorption of Pb^{2+} from aqueous solution using coconut and palm kernel shells was investigated. The morphological features of the shells were studied using the energy dispersive X-ray spectroscopy, scanning electron microscopy, X-ray diffraction spectroscopy and Fourier transform infrared spectroscopy. Equilibrium, kinetic and thermodynamic batch adsorption experiments were carried out by the concentration, time and temperature effects respectively. The morphological images of the shells showed irregular small size particles which indicated a high surface area and porosities that facilitated sorption. The adsorption studies recorded relatively rapid uptake of Pb^{2+} by the shells which were mainly kinetic controlled and followed a second order process. The thermodynamic studies suggested relatively low temperature (low energy) favoured sorption which was exothermic with both physisorption and chemisorption mechanisms for both shells.

Keywords: Sorption, Coconut, Palm kernel shell, Adsorbent, Heavy metals, comparative.

INTRODUCTION

Lead in our environment resulting from many industrial activities such as tannery, mining, alloying, battery production, *etc*. has significantly had major health impacts on humans and other organisms[1]. In recent years, the surge of industrial activities has intensified more environmental problems as, for example in the deterioration of several ecosystems due to the accumulation of dangerous pollutants such as lead[2]. There is, therefore, the need for the removal of these toxic metal ions from municipal, commercial and industrial effluents before discharge into the environment. The conventional methods of removal of heavy metals from waste water which include precipitation, flocculation, filtration, ion exchange, reverse osmosis, *etc.*, are very much capital intensive. However low-cost and renewable materials have been used for the removal of metals from effluents which include biomasses like Nipa palm, *Manihot sculenta Cranz*, Sea weed and *Medicago sativa*[3-6]. There is the need a further search for more low-cost and locally available adsorbent materials with maximum adsorption capacity.

Information on the uses of coconut and palm kernel shells for the removal of metal ions from solutions is scanty which has necessitated the present comparative study.

Coconuts are the seeds of a species of palm called *Cocos nucifera* which belongs to the arecaceae family and found throughout the tropic and sub-tropic area where it is known for its versatility. The palms flower on a monthly basis and the fruit take one year to ripen. A mature tree may have fruit in every stage of maturity and can produce 50 to 100 coconuts per year[7,8]. The fruit contains the fibrous layer, the hard shell and the inner edible whitish layer (endosperm). The fibrous layer can be separated from the hard shell manually. The hard shell is broken open to separate it from the nutritious edible endosperm[9,10]. Large quantities of coconut shell are generated annually and only some fractions are used for fuel and some other applications, but greater percentage are dumped around the processing mill constituting environmental and economic liability for the people[8]. Coconut shell is composed of 53.06 % cellulose, 36.51 % lignin and 29.27 % pentosans[11]. Coconut shell powder is used to produce shell charcoal and applied widely as domestic and industrial fuel. Shell charcoal is used to produce activated carbon. Activated carbon produced from coconut shell has certain specific advantages as the raw material can adsorb certain molecular species. Coconut shell powder is also used as fillers in the manufacture of thermosets.

Elaeis guineensis (oil palm) originated in Guinea and was later introduced to Java (Indonesia), Nigeria and Malaysia. Though the oil palm originated in West Africa, it has since been planted successfully in tropical regions within 20 degrees of the equator[12,13]. Oil extracted from both the pulp of the fruit (palm oil) and the kernel (palm kernel oil) is used for foods

and soap manufacture[14]. The increasing use of oil in the commercial food industry all over the world is because of its cheap pricing, high oxidative stability and high levels of natural antioxidants[15].

Palm kernel is a virgin biomass with high calorific value, low ash, moisture and sulphur contents. It is a lignocellulose biomass. Carbonized palm kernel shells are used as charcoal which can be pressed into bio-fuel briquette. It can also be processed into activated carbon which is used in liquid and gas phase filtration or adsorption[16]. In 2010/2011, the total world production of palm kernels was 12.6 million tons[17].

EXPERIMENTAL

Shell samples were obtained from the waste bins and thoroughly washed with the deionized water and oven dried at 30 °C . The dry samples were ground and passed through the 100-mesh screens using a Wiley mill. These particle sizes were then washed twice with 0.01 M HCl to remove any metals and debris that might be in the shells prior to experimental metal ion exposure. The acid washed shell samples were washed twice again with deionized water to remove acid and then oven dried at 30 °C to constant weight.

Characterization of shell sample: The morphological features of the shells were analyzed by FE-SEM, EDS, XRD and FTIR. The surface morphology and EDS measurements were recorded with a JEOL 7500F Field Emission scanning election microscope. Powder X-ray diffraction (PXRD) patterns were collected with a bruker AXS D8 Advanced diffractometer operated at 45 kv and 40 mA with monochromated copper Kα1 radiation wavelength (λ = 1.540598) and Kα2 radiation wavelength (λ = 1.544426). Scan speed of s/step and step size of 0.03°. IR spectra were recorded using Perkin-Elmer spectrum 400 FTIR/FT-NIR spectrometer in the range 4000-400 cm^{-1}.

Batch adsorption experiment

Concentration effect: 0.2 g of the shell samples were weighed and placed in pre-cleaned test tubes. Six metal ion solutions with standard concentrations of 21.8, 48.0, 72.3, 97.7, 120.9 and 141.5 mg/L were made from spectroscopic grade standards of Pb^{2+} [from $Pb(NO_3)_2$]. 10 mL of each metal solution were added to each tube containing the shells and equilibrated for 1 h by shaking at 29 °C. The shell suspensions were centrifuged for 5 min at 2500 rpm. The supernatants were analysed as stated in metal analysis. The amount of metal uptake was computed using eqn. 1.

Time dependent studies: 0.2 g of the shell samples were weighed and placed in five pre-cleaned test tubes. Metal ion solution with standard concentration of 72.3 mgL was made from spectroscopic grade standard of Pb^{2+} [from $Pb(NO_3)_2$]. 10 mL of the metal solution was added to each tube containing the shell sample and equilibrated for each time intervals of 5, 10, 20, 40 and 60 min, respectively by shaking at 29 °C. The shell suspensions were centrifuged for 5 min at 2500 rpm. The supernatants were analysed as stated in metal analysis. The amount of metal uptake was computed using equation 1.

Temperature effect: 0.2 g of the shell samples were weighed and placed in four pre-cleaned test tubes. Metal ion solution with standard concentrationof 72.3 mg/L was made from spectroscopic grade standard of Pb^{2+}. 10 mL of the metal solution was added to each tube containing the shell sample and equilibrated for 1 h by shaking at temperatures of 28, 40, 60 and 80 °C, respectively using a Compenstat Gallenhamp water bath. The shell suspensions were centrifuged for 5 min at 2500 rpm. The supernatants were analysed as stated in metal analysis. The amount of metal uptake was computed using eqn. 1.

Metal analysis: The metal analysis was performed by AAS using a Buck Scientific Atomic Absorption/Emission spectrophotometer 200A (AAES). Controls of one of the metal solution were run to detect any possible metal precipitation or contamination.

Data analysis: Various equilibrium, kinetic and thermodynamic models (equations) were employed to interpret the data and establish the extent of adsorption. The amount of metal uptake was computed using the material balance equation for batch dynamic studies[5] (eqn. 1).

$$q_e = \frac{V}{M}(C_o - C_e) \quad (1)$$

with q_e as metal uptake capacity ($\left(\frac{mg}{l}\right)$ shell at equilibrium), C_e is metal ion concentration in solution $\left(\frac{mg}{l}\right)$ at equilibrium, C_o, the initial metal ion solution $\left(\frac{mg}{l}\right)$, V, the volume of solution in litres and M, the dry weight of shell used in (g).

Langmuir plots were carried out using the linearized eqn. 2 below

$$\frac{M}{X} = \frac{1}{abC_e} + \frac{1}{b} \quad (2)$$

where is the amount of Pb^{2+} adsorbed per mass M of shell in $\frac{mg}{l}$, a and b are the Langmuir constants obtained from the slope and intercepts of the plots.

The essential characteristics of the Langmuir isotherm were expressed in terms of a dimensionless separation factor or equilibrium parameter[18] S_f.

$$S_f = \frac{1}{(1 + aC_o)} \quad (3)$$

with C_o as initial concentration of Pb^{2+} in solution Poot *et al.*[18] have shown by mathematical calculations that the magnitude of the parameter S_f provides a measure of the type of adsorption isotherm. $I_f > 1$, the isotherm is unfavourable; $S_f = 1$ (linear); $0 < S_f < 1$ (favourable) and $S_f = 0$ (irreversible).

The adsorption intensity of the Pb^{2+} in the shell was assessed from the Freundlich plots using the linearized eqn. 4 below

$$\ln\frac{X}{M} = \frac{1}{n}(\ln C_e) + \ln K \quad (4)$$

where K and *n* are Freundlich constants and $\frac{1}{n}$ is approximately equal to the adsorption capacity.

The fraction of shell surface covered by the Pb^{2+} was computed using eqn. 5

$$\theta = 1 - \frac{C_e}{C_o} \quad (5)$$

where θ is the degree of surface coverage.

The effectiveness of the adsorbent (shell) was assessed by the number of cycles of equilibrium sorption process required to reduce the levels of Pb^{2+} in solution according to the value of the distribution (partition coefficient[19] (K_d) in eqn. 6.

$$K_d = \frac{C_{aq}}{C_{ads}} \quad (6)$$

where is concentration of Pb^{2+} in solution, $\frac{mg}{l}$; C_{ads} is concentration of Pb^{2+} in shell in $\frac{mg}{l}$.

The heat of adsorption (Q_{ads}) was obtained using the following[20] Suzuki eqn. 7.

$$\ln \theta = \frac{\ln K_0 C_o}{T^{0.5}} + \frac{Q_{ads}}{RT} \quad (7)$$

where T as solution temperature (K); K_0 a constant and R gas constant (8.314 $Jmol^{-1} K^{-1}$).

The linear form of the modified Arrhenius expression was applied to the experimental data to evaluate the activation energy (E_a) and sticking probability S* as shown[21] in eqn. 8.

$$\ln (1 - \theta) = S^* + \frac{E_a}{RT} \quad (8)$$

The apparent Gibbs free energy of sorption ΔG° which is a fundamental criterion for spontaneity, was evaluated using the following eqn. 9.

$$\Delta G° = -RT \ln K_0 \quad (9)$$

where K_0 is obtained from the Suzuki eq. 7.

The experimental data was further subjected to thermodynamic treatment in order to evaluate the apparent enthalpy (ΔG°) and entropy (ΔS°) of sorption using eqn. 10.

$$\ln K_o = \frac{\Delta S°}{R} - \frac{\Delta H°}{RT} \quad (10)$$

To evaluate the packing of Pb^{2+} on the shell surface, thermodynamic analysis of adsorption density (ρ) was carried out with the following eqn. 11.

$$\rho = ZrC_e e^{-(\Delta G°/RT)} \quad (11)$$

where is the valency of the Pb^{2+}, r the effective radius of the Pb^{2+} in cm and C_e the equilibrium concentration in mol/cm^3.

The expression relating the number of hopping (n) and that of the surface coverage (θ) as shown in eqn. 12 was applied to the experimental data.

$$n = \frac{1}{(1 - \theta)\theta} \quad (12)$$

Other thermodynamic parameters such as adsorption potential (A) was tested by applying eqn. 13.

$$A = -RT \ln \frac{C_o}{C_e} \quad (13)$$

with C_o and C_e as initial and equilibrium concentrations in, mol/cm^3 R, the gas constant and T, the solution temperature in K.

The kinetic behaviour of the sorption process was investigated by testing the data using the second order kinetic model expressed in eqn. 14.

$$\frac{1}{q_t} = \frac{1}{q_o} + K_2 \quad (14)$$

where q_t is the amount of Pb^{2+} on the shell (mg/g or mmol/g) at time t, q_o is the amount of Pb^{2+} on the shell at time to and is the second order rate constant.

RESULTS AND DISCUSSION

Fourier transform infrared (FT-IR) spectroscopic study of the shells was carried out to determine the active functional groups responsible for the binding of Pb^{2+} from solution. FTIR spectrum of coconut and palm kernel are presented in Fig. 1a,b. The FTIR spectra of coconut and palm kernel shells, Fig. 1a,b. The sharp peaks at 1600-1200 cm^{-1} due to the C-H stretching, 1300-1000 cm^{-1} due to the C-O stretching, 1500-1300 cm^{-1} due to the C-H bending, 3500-2500 cm^{-1} due to free O-H stretching, 1400-1200 cm^{-1} due to C-O-C stretching and 1400-1100 cm^{-1} due to O-H bending for coconut shell and 1600-1200 cm^{-1} due to the C-H stretching, 1300-1000 cm^{-1} due to the C-O stretching , 1500-1300 cm^{-1} due to the C-H bending, 3500-2500 cm^{-1} due to free O-H stretching, 1400-1200 cm^{-1} due to C-O-C stretching and 1400-1100 cm^{-1} due to O-H bending in the shells, the presences of these absorption bands indicate that no functional groups may have played a major role in the sorption process.

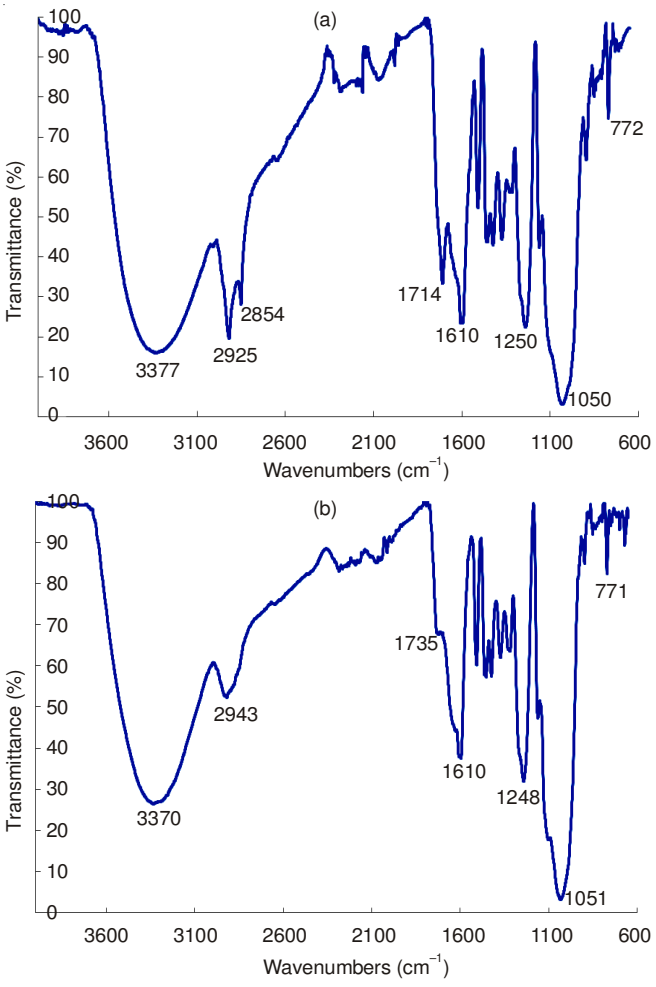

Fig. 1. Fourier transform infrared (FTIR) spectra of (a) coconut and (b) palm kernel shells

X-ray powder diffraction is a powerful tool for characterizing a solid state sample. Each crystalline species has a unique X-ray diffraction pattern. With a diffraction pattern an investigator can identify an unknown specie or characterize the atomic scale structure of an already identified substance. The XRD diffractogram of coconut and palm kernel shells are presented in Fig. 2a,b. The most prominent peak in the shells are observed at 2θ = 21.69 and 21.04 for coconut and palm kernel shell, respectively. The presences of these diffraction peaks indicate these shells to be amorphous rather than crystalline in nature.

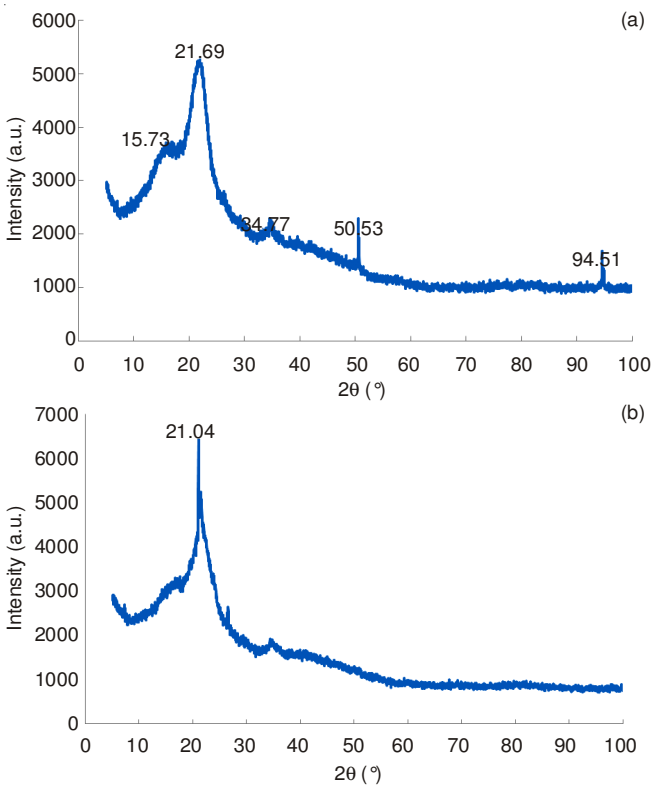

Fig. 2. X-Ray diffraction patterns of (a) coconut and (b) palm kernel shells

Energy dispersive X-ray (EDX) was applied for elemental analysis of the shell samples. The EDX spectra of the coconut and palm kernel shells are presented in Fig. 3a, b. The spectra indicate peaks due to the following elements: C (10 %), Ca (40 %), O (50 %) for coconut and C (51 %), Ca (1 %), O (48 %) for palm kernel in addition to hydrogen. The presence of these elements will produce charges and functional groups on the surface of the shells and create electrostatic forces of attraction between the samples and Pb^{2+} in solution.

In order to determine the morphology of the shells, scanning electron microscope (SEM) images of the samples were taken at magnification × 270. The SEM images of the coconut and palm kernel shells are presented in Fig. 4a, b. The SEM images show that the surfaces of the shell samples had irregular small size particles which indicated a high surface areas and porous nature as shown in Fig. 4. Large surface area of any adsorbent facilitates maximum adsorption[20].

The percentage sorption of Pb^{2+} by the shells at different concentrations of the Pb^{2+} are presented in Fig. 5. The maximum adsorption of 94 % took place at equilibrium concentration

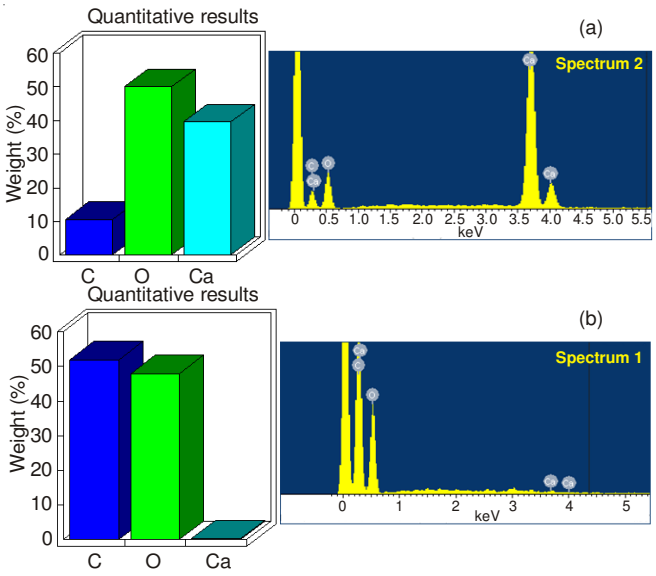

Fig. 3. Energy dispersive X-ray (EDX) of the shells showing quantitative results and spectra of (a) coconut and (b) palm kernel shells

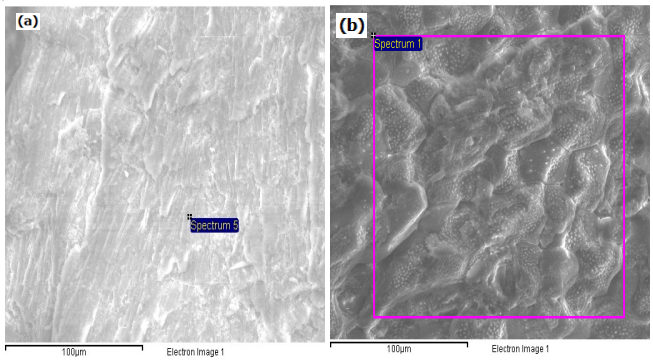

Fig. 4. Scanning electron microscope (SEM) images of (a) coconut and (b) palm kernel shells

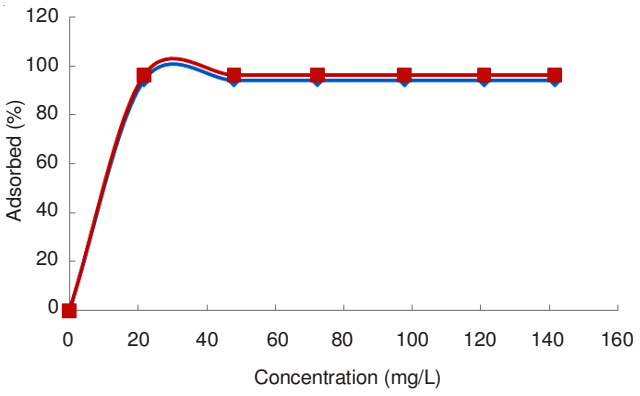

Fig. 5. Effect of initial concentration on the sorption of Pb^{2+} by the shells: ◆ coconut and ■ palm kernel

of 20 mg/L Pb^{2+} for coconut shell and of 96 % at equilibrium concentration of 20 mg/L Pb^{2+} for palm kernel. This is because at lower concentration more shell sites were available for the Pb^{2+}, but as the concentration of Pb^{2+} increased, the adsorption capacity of the shells decreased due to reduced availability of free pore spaces and sites. The results indicated that the sorption of Pb^{2+} were very much dependent on the concentration of the Pb^{2+}.

Time dependency studies show the amount of time needed for maximum adsorption to occur. The variation in percentage removal of Pb^{2+} with time has been presented in Fig. 6. It indicates that a maximum of 93 % removal of Pb^{2+} was observed in 5 min and remained constant afterwards for coconut shell and 99 % within 5 min for palm kernel shell. The relatively short contact times required to attain equilibrium suggest that rapid uptake of Pb^{2+} by the shells occurred to fill some of the vacant pores and sites in the shells and after which the remaining spaces were difficult to be occupied due to repulsive forces between the Pb ions.

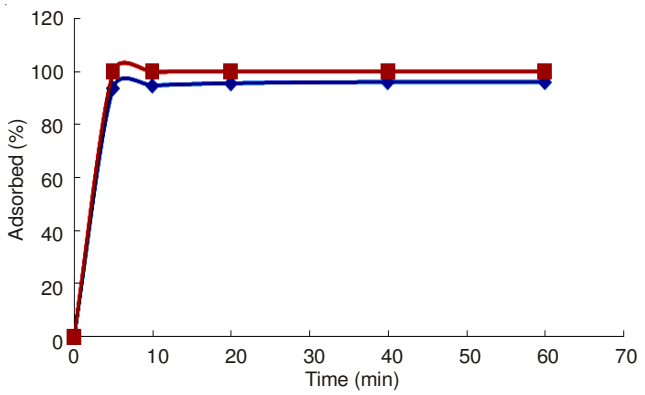

Fig. 6. Effect of contact time on the sorption of Pb^{2+} by the shells: ◆ coconut and ■ palm kernel

Fig. 7 presents the plot of percentage adsorption of Pb^{2+} by the shells at varying temperatures with optimum sorption of 93 % occurring at 28 °C for the coconut shell and 95 % at 30 °C for palm kernel shell. The plots showed that further increase in temperature resulted in a slight decrease in adsorption. This is in agreement with the general principle that physical adsorption decreases with increase in temperature, *i.e.*, molecules adsorbed earlier on a surface tend to desorb from it at elevated temperatures[22]. This behaviour could be attributed to the weakening of the attractive forces between the shells and Pb^{2+}, the increased kinetic energy of the Pb^{2+} and the decrease in the thickness of the boundary layers of the shells due to the higher tendency of the Pb^{2+} to escape from the shells.

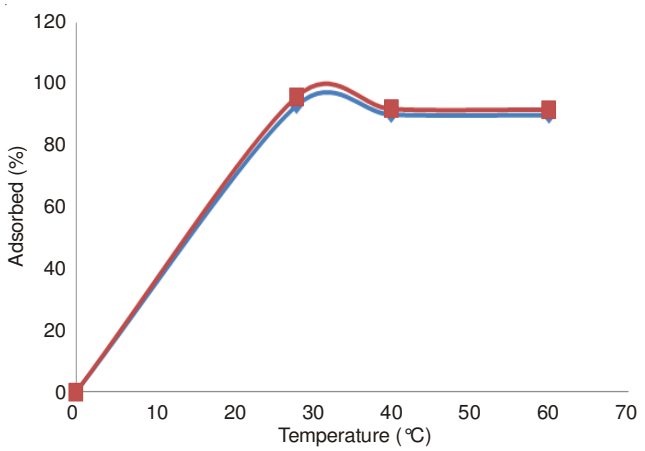

Fig. 7. Effect of temperature on the sorption of Pb^{2+} by the shells: ◆ coconut and ■ palm kernel

The extent of adsorption can be correlated by means of an isotherm. Attempts were made to fit the data obtained from the adsorption experiments into various adsorption isotherms. The linear plots of the Langmuir and Freundlich isotherm models for the sorption of Pb^{2+} by the shells are presented in Figs. 8a,b and 9a,b. These straight line plots confirmed the application of the Langmuir and Freundlich isotherm models to the adsorption of Pb^{2+} by the shells. The slopes and intercepts were used to compute the Langmuir constants and adsorption capacity.

The fraction of the shell surfaces covered by the Pb^{2+} is given as 0.941 for coconut and 0.962 for palm kernel (Table-1). These values indicate that over 94 and 96 % of the pore spaces of the coconut and palm kernel shell surfaces respectively were covered by the Pb^{2+}, which means higher degree of adsorption with the palm kernel shell.

In order to determine the nature of the adsorption process, whether favourable or unfavourable, the dimensionless constant separation term S_f was investigated (eqn. 3). The result (S_f = 0.999) for coconut shell and (S_f = 0.00018) for the palm kernel shell, in Table-1 were less than one and greater than zero which showed that the sorption of Pb^{2+} onto the shells was favourable.

The effectiveness of the shells as adsorbents for Pb^{2+} from solution was assessed through the sorption distribution or partition coefficient presented in Table-1. The value of (0.062) for coconut shell and (0.039) for palm kernel shell suggest that palm kernel shell is a more effective adsorbent than coconut shell and that a few number of cycles of equilibrium sorption process will be required to reduce the levels of Pb^{2+} in solution.

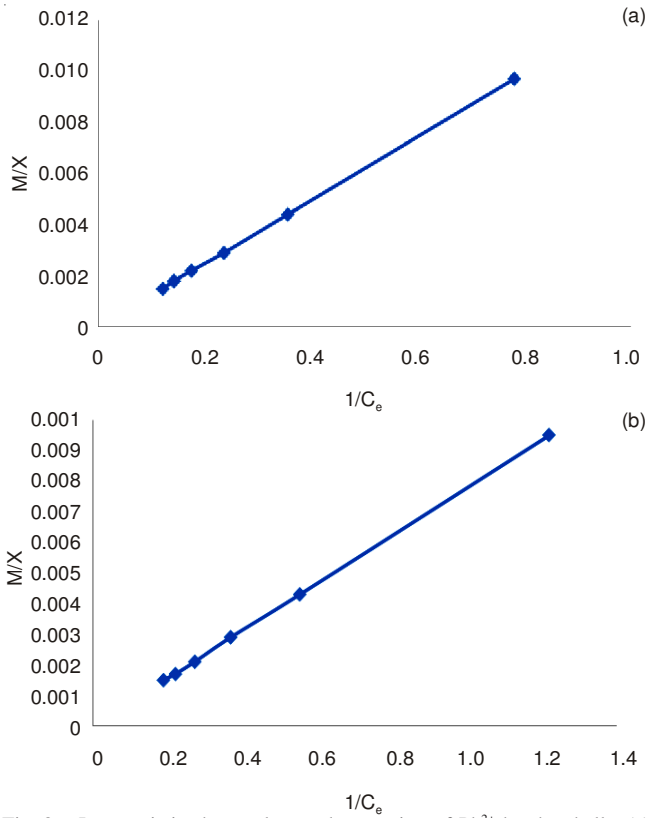

Fig. 8. Langmuir isotherm plot on the sorption of Pb^{2+} by the shells, (a) coconut and (b) palm kernel

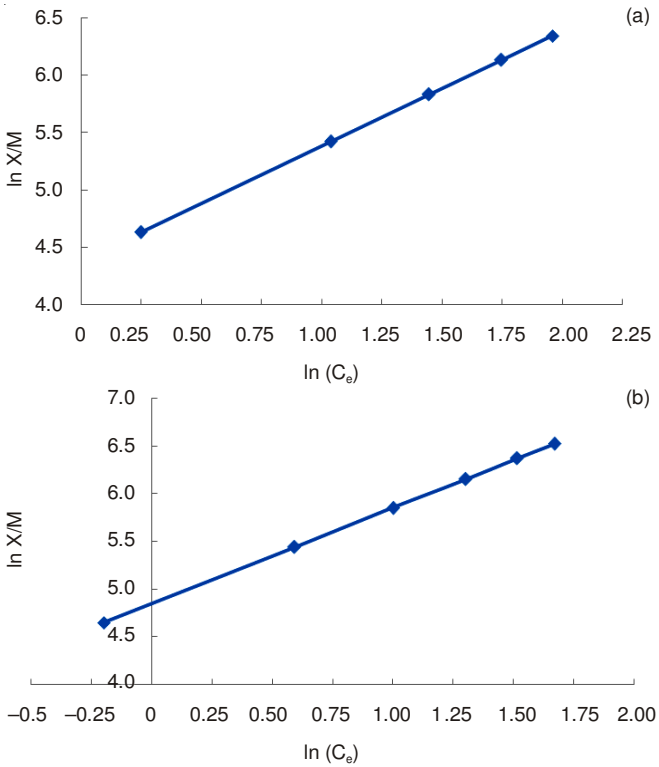

Fig. 9. Freundlich isotherm plot on the sorption of Pb^{2+} by the shells, (a) coconut and (b) palm kernel

TABLE-1
EQUILIBRIUM AND KINETIC PARAMETERS

Shells	Rate constant ($K\ min^{-1}$)	Surface coverage (θ)	Separation factor (S_f)	Sorption coefficient (K_d)	Adsorption capacity (mol/g)
Coconut	5.0×10^{-5}	0.941	0.999	0.062	1.00
Palm kernel	7.2×10^{-4}	0.962	0.00018	0.039	1.01

From the Freundlich plot (Fig. 9a,b), the adsorption capacities of the shells were calculated to be 1 mol/g for coconut shell and 1.01 mol/g for palm kernel shell.

In order to calculate the heats of adsorption (Q_{ads}) for the sorption of Pb^{2+} onto the shells, eqn. 7 was used. The value of (-26.94 KJ $mol^{-1}K^{-1}$) for coconut shell and (-32.96 KJ $mol^{-1}K^{-1}$) for palm kernel shell are negative as presented in Table-2, which indicate that the adsorptions were exothermic i.e., low temperatures favour the adsorption of Pb^{2+} by the shells and also suggested kinetic controlled second order processes. Temperature increase did not enhance the sorption processes.

The plots of ln(1-θ) *vs.* 1/T using eqn. 8 yielded straight lines as presented in Fig. 10. The activation energies E_a and the sticking probabilities E_a and S* were calculated from the slopes and intercepts, respectively. The values of E_a and S* were shown in Table-2 as coconut (-30.07 $Jk^{-1}mol^{-1}$), palm

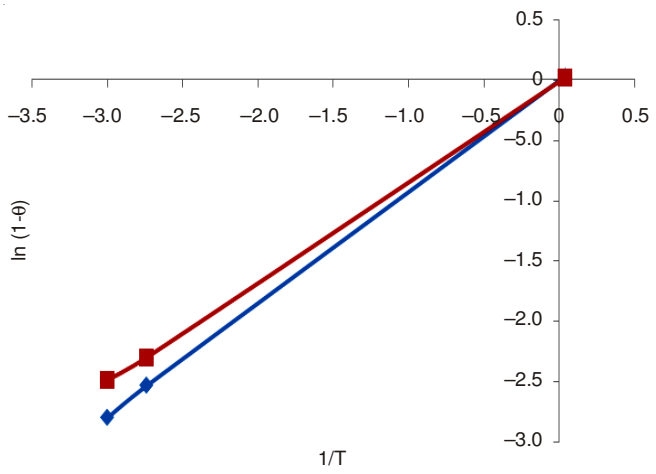

Fig. 10. Plot of ln(1-θ) *vs.* 1/T on the sorption of Pb^{2+} by the shells: ◆ coconut and ■ palm kernel

kernel (-298.0 $Jk^{-1}mol^{-1}$) and coconut (1), palm kernel (1), respectively. The relatively low and negative E_a values indicate that low temperature or energy favours the sorption and the adsorption processes were exothermic. Relatively high values also suggest that the sorption processes were kinetic controlled. The sticking probability S* indicates the measure of the potential of an adsorbate to remain on the adsorbent. It is often interpreted as S* > 1 (no sorption), S* = 1 (mixture of physisorption and chemisorption), S* = 0 (indefinite sticking-chemisorption), 0 < S* < 1 (favourable sticking-physisorption). The values of S* obtained for the sorption of Pb^{2+} by the shells were one which indicate that the adsorption was favourable and followed both physisorption and chemisorption mechanisms.

Table-2 also presents the Gibbs free energy ΔG° for the sorption of Pb^{2+} by the shells which was calculated from eqn. 9. Gibbs free energy is the fundamental criterion of spontaneity. The ΔG° value of -6.116 KJ/mol for coconut shell and -6.951 KJ/mol for palm kernel were negative indicating that the sorption processes were spontaneous. The values obtained for ΔG° were also less than -20 KJ/mol suggesting electrostatic interactions between the Pb^{2+} and the shells which supported occurrence of physisorption mechanism in addition to the chemisorption.

The plots of lnK_o *vs.* 1/T from eqn. 10 were linear as presented in Fig. 11, with the slopes and intercepts equal to -ΔH°/R and ΔS°/R, respectively. The values of the enthalpy changes (ΔH°) calculated from the slopes were coconut (-0.111 J/mol) and palm kernel (-325.0 J/mol). The negative ΔH° values suggest that sorption proceeded favourably at a lower temperatures and the sorption mechanisms were exothermic. The values of the entropy changes computed from the intercept were coconut (-14.13 J/mol K), palm kernel (-14.14 J/mol K)

TABLE-2
THERMODYNAMIC PARAMETERS

Shells	Heat of adsorption (Q_{add} KJ/Kmol)	Sticking probability (S*)	Activation energy (E_a J/Kmol)	Gibbs free energy of adsorption (ΔG° KJ/mol)	Apparent entropy (ΔG° JK/mol)	Apparent enthalpy (ΔH° J/mol)	Adsorption density (P mol/cm^2)	Hopping number (n)	Adsorption potential (A KJ/mol)
Coconut	-26.94	1.00	-30.07	-6.116	-14.13	-0.111	7.03×10^{-5}	11	6.37
Palm kernel	-32.96	1.00	-298.0	-6.951	-14.14	-325.0	8.17×10^{-5}	13	7.15

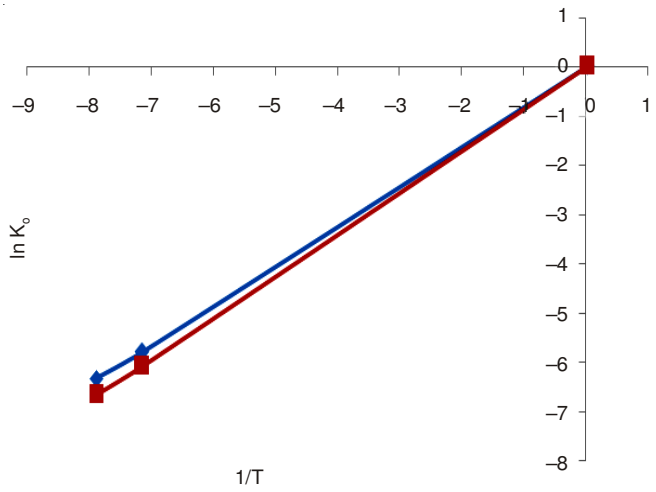

Fig. 11. Plot of $\ln K_o$ *vs.* 1/T on the sorption of Pb^{2+} by the shells: ◆ coconut and ■ palm kernel

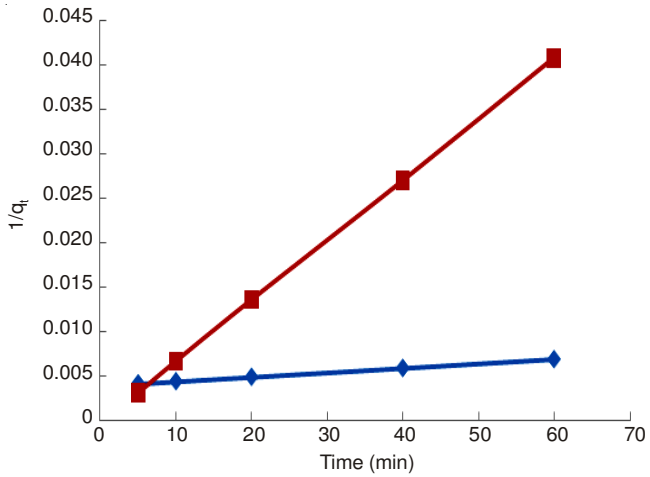

Fig. 12. Second order kinetic plot on the sorption of Pb^{2+} by the shells: ◆ coconut and ■ palm kernel

and presented in Table-2. The negative ΔS values obtained suggest that the freedom of the adsorbed Pb^{2+} were comparably restricted in the samples, indicating that chemisorption mechanism predominates.

The packing of Pb^{2+} in the shells was assessed using eqn. 11 and results presented in Table-2. The adsorption densities, ρ, obtained were 7.03×10^{-5} and 8.17×10^{-5} for coconut and palm kernel, respectively.

The changes in the chemical potentials that occurred as the Pb^{2+} removed from the solution to the surfaces of the shells were calculated using eqn. 13. Table-2 give the adsorption potentials as coconut (6.37 KJ/mol) and palm kernel (7.15 KJ/mol).

The probability of Pb^{2+} finding vacant site on the shell surfaces during the sorption was correlated by the number of hopping (n) done by the Pb^{2+}. The hopping numbers presented in Table-2 were 11 and 13 for coconut and palm kernel, respectively. The lower the hopping number the faster the adsorption[21]. The relatively low value of nobtained for both shells suggests that the adsorption of Pb^{2+} was fast.

The rate at which sorption takes place in a batch sorption process is very important in designing batch sorption systems. Consequently, it was important to establish the time dependence of such system under various process conditions. In an attempt to understand the sorption process, the second order kinetic rate expression model was applied to the experimental data. The second order kinetic model was applicable to the experimental data because linear relationships were obtained by the plots of t/q_t *versus* t as presented in Fig. 12.

Conclusion

The equilibrium, kinetic and thermodynamic studies recorded relatively rapid uptake of Pb^{2+} by the coconut and palm kernel shells which were kinetic controlled second order processes. The adsorptions were favoured by low temperature and energy which were exothermic with both physisorption and chemisorption mechanisms. The shells were effective adsorbent for the removal of Pb^{2+} from aqueous solution. The results from this study will be useful for a novel filtration technology which is effective and environment friendly to remove and recover heavy metals from aqueous solutions. This will replace the most conventional relatively expensive treat-ment techniques presently in existence, which are not economically viable for small scale industries due to huge capital investment.

ACKNOWLEDGEMENTS

This work was supported by a research grant from the Research Directorate of the Vaal University of Technology Vanderbijlpark, South Africa.

REFERENCES

1. K. Kadirvelu, C. Faur-Brasquet and P.L. Cloirec, *Langmuir*, **16**, 8404 (2000).
2. D. Park, Y. Yun, J.H. Jo and J.M. Park, *Ind. Eng. Chem. Res*., **45**, 5059 (2006).
3. D. Wankasi, Ph.D. Thesis, Kinetics of Phytosorption of Heavy Metals Using Unmodified and Modified Biomass Nipa Palm (*Nypa fruticans Wurmb*), University of Port Harcourt, Nigeria (2004).
4. M. Horsfall Jnr and A.I. Spiff and A.A. Abi, *Bull. Korean Chem. Soc*., **25**, 967 (2004).
5. K.H. Chu and M.A. Hashim, *Acta Biotechnol*., **21**, 295 (2001).
6. J.L. Gardea-Torresdey, J.H. Gonzalez, K.J. Tiemann, O. Rodriguez and G. Gamez, *J. Hazard. Mater*., **57**, 29 (1998).
7. Webster's Online Dictionary (http://www.websers-online-dictionary.org).
8. T. Woolley, S. Kimmins, P. Harrison and R. Harrison, Green Building Handbook, A Guide to Building Products and Their Impact on the Environment, Green Building Digest, Spon Press, ISBN 0-419-22609-7, Vol. 1 (1997).
9. S. Piniappan, The Mystery Behind Coconut Water, The Hindu (2002).
10. T. Predeepkumor, B. Sumajiyothibkaskar and K.N. Satheesan, Management of Horticultural Crops, (Horticulture Science Series), New India Publishing, Vol. 11, pp. 539-587 (2008).
11. R. Child, *J. Am. Chem. Soc*., **60**, 1506 (1938).
12. F.I. Obahiagbon, *Am. J. Biochem. Mol. Biol*., **2**, 106 (2012).
13. R.H.V. Corley and C.H. Lee, *Euphytica*, **60**, 179 (1992).
14. R.R.M. Paterson, *J. Crop Prot*., **26**, 1369 (2007).
15. B.C. Man, J.L. Liu, B. Jamilah and R.A. Rahman, *J. Food Lipids*, **6**, 181 (1999).
16. B. Mathaus, *Eur. J. Lipid Sci. Technol*., **109**, 400 (2007).
17. Food outlook, FAO Org., Food and Agriculture Organization of the United Nations May 2012, Retrieved August 2012.
18. V.J.P. Poots, G. Mckay and J.J. Healy, *J. Water Pollut. Control Fed*., **50**, 926 (1978).
19. D. Wankasi, M. Horsfall and A.I. Spiff, *Chem. Tech. J*., **4**, 54 (2006).
20. M Suzuki, Adsorption Engineering, Kodanasha/Elsevier, Tokyo/Amsterdam, pp. 71-73 (1990).
21. D. Wankasi, Adsorption, A Guide to Experimental Data Analysis, Ano Publication Company, Nigeria, pp. 40-43 (2013).
22. D. Wankasi, M. Horsfall Jnr and A.I. Spiff, *Afr. J. Biotechnol*., **4**, 923 (2005).